Figures and figure supplements

Cross-talk between individual phenol-soluble modulins in *Staphylococcus aureus* biofilm enables rapid and efficient amyloid formation

Masihuz Zaman and Maria Andreasen

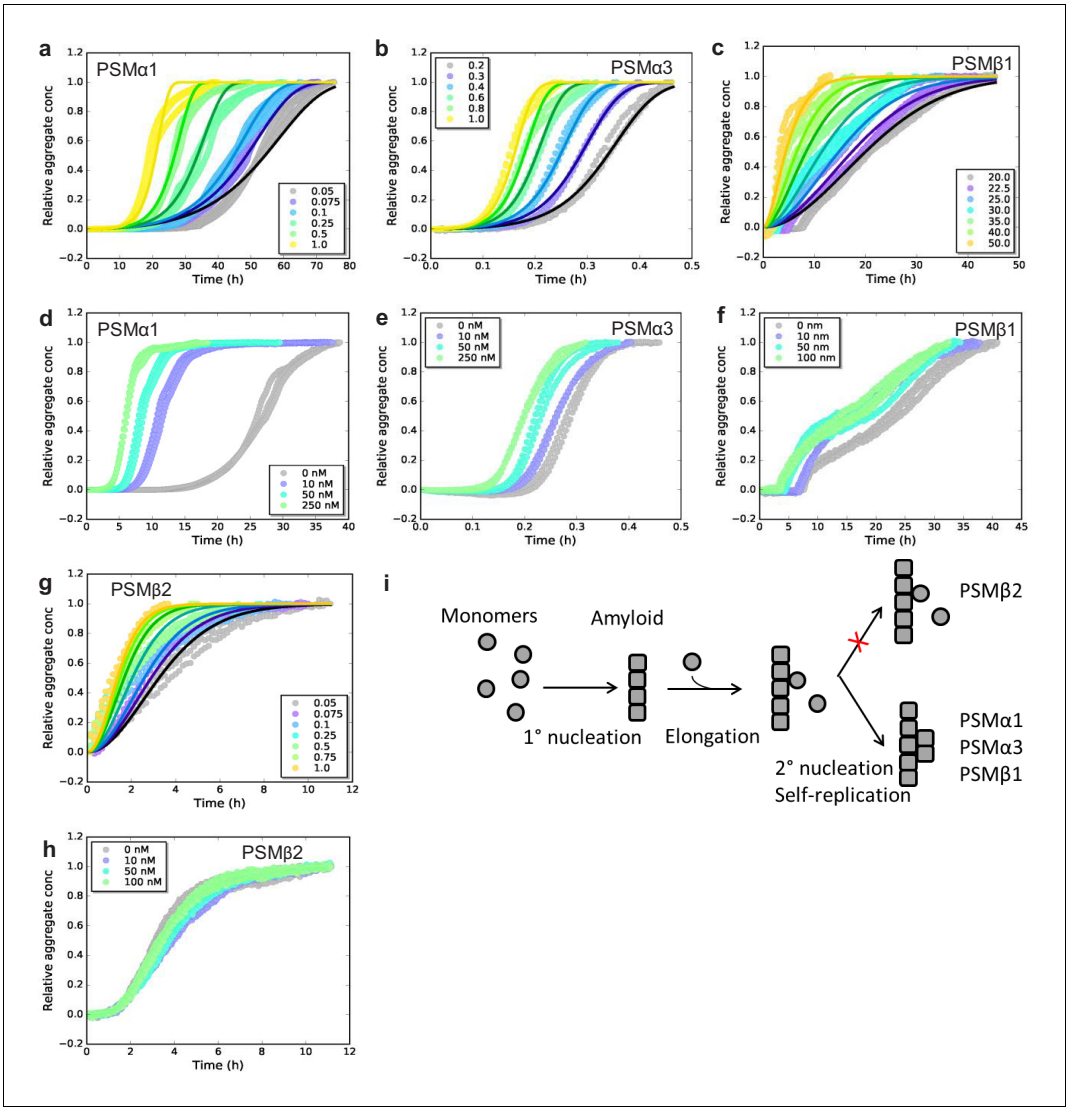

Figure 1. Experimental kinetic data for the aggregation of phenol-soluble modulin (PSMs) peptides from monomeric peptides. (**a**) Aggregation of PSMα1 (0.05–1.0 mg/mL) fitted to a secondary nucleation model. (**b**) Aggregation of PSMα3 (0.2–1.0 mg/mL) fitted to a secondary nucleation model. (**c**) Aggregation of PSMβ1 (20–50 µg/mL) fitted to a secondary nucleation model. (**d**) Aggregation of PSMα1 in the presence and absence of low concentrations of preformed seeds (monomers: 0.5 mg/mL, seeds: 0–250 nM). Significant effects on the rate of aggregation were observed. (**e**) Aggregation of PSMα3 in the presence and absence of low concentrations of preformed seeds (monomers: 0.4 mg/mL, seeds: 0–250 nM). Significant effects on the rate of aggregation were observed. (**f**) Aggregation of PSMβ1 in the presence and absence of low concentration of preformed seeds (monomers: 0.025 mg/mL, seeds: 0–100 nM). Significant effects on the rate of aggregation were observed. (**g**) Aggregation of PSMβ2 (0.05–1.0 mg/mL) fitted to a nucleation-elongation model. (**h**) Aggregation of PSMβ2 in the presence and absence of low concentration of preformed seeds (monomers: 0.05 mg/mL, seeds: 0–100 nM). No significant effects on the rate of aggregation are evident. (**i**) Schematic illustration of the microscopic steps in PSM aggregation. Monomers of PSMβ2 nucleate through primary nucleation (rate constant: k_n) and the aggregates grow by elongation (rate constant: k_+). Additionally monomers of PSMα1, PSMα3, and PSMβ1 nucleate through secondary nucleation on the surface of already existing aggregate (rate constant: k_2). All kinetic experiments were carried out in triplicates. Parameters from the data fitting are summarized in ***Table 1***.

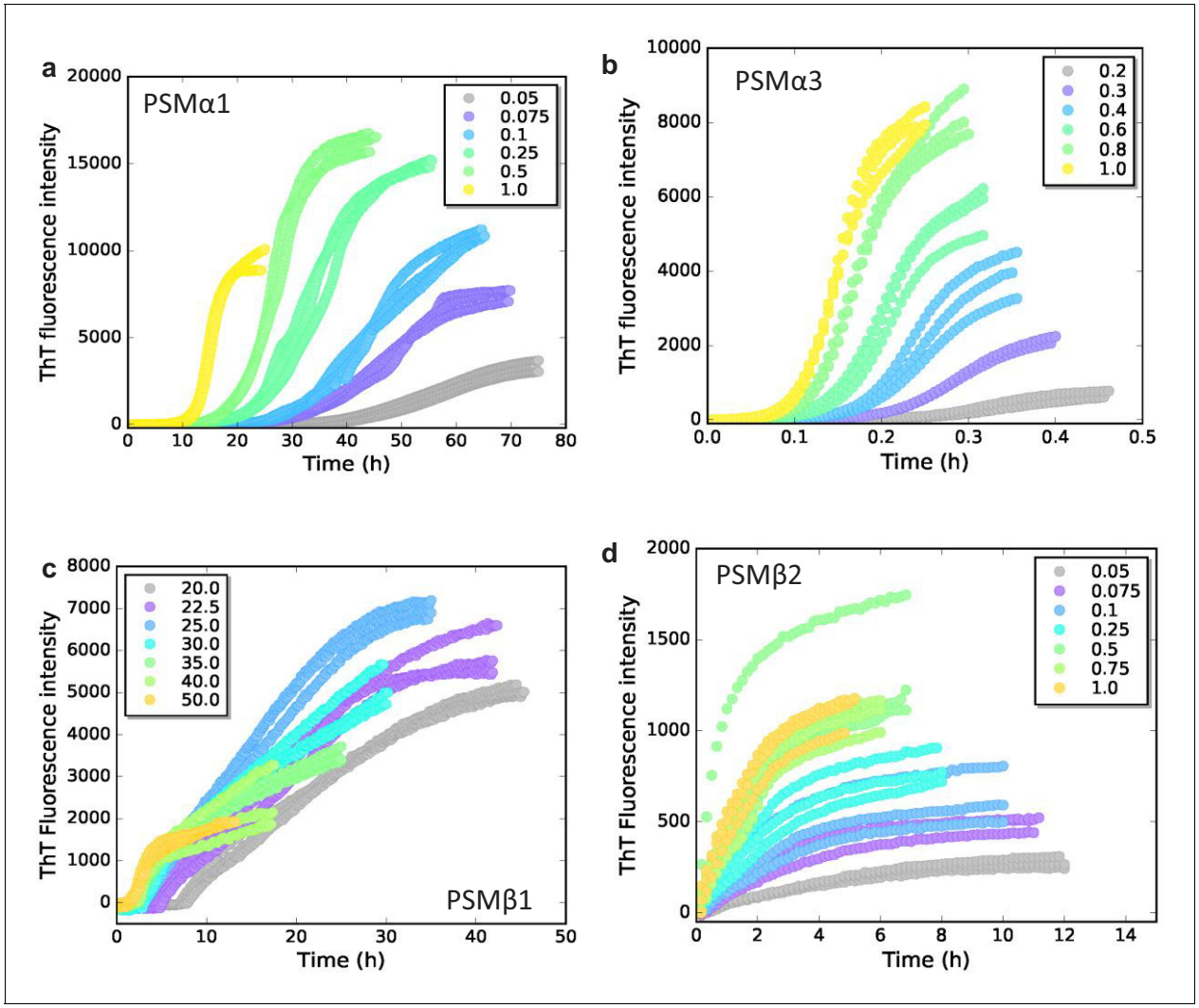

Figure 1—figure supplement 1. Experimental kinetic raw data. Raw ThT fluorescence data for the aggregation of the phenol-soluble modulin (PSM) peptides under quiescent conditions at 37°C. (**a**) Aggregation of PSMα1 (0.05–1.0 mg/mL). (**b**) Aggregation of PSMα3 (0.2–1.0 mg/mL). (**c**) Aggregation of PSMβ1 (20–50 µg/mL). (**d**) Aggregation of PSMβ2 (0.05–1.0 mg/mL).

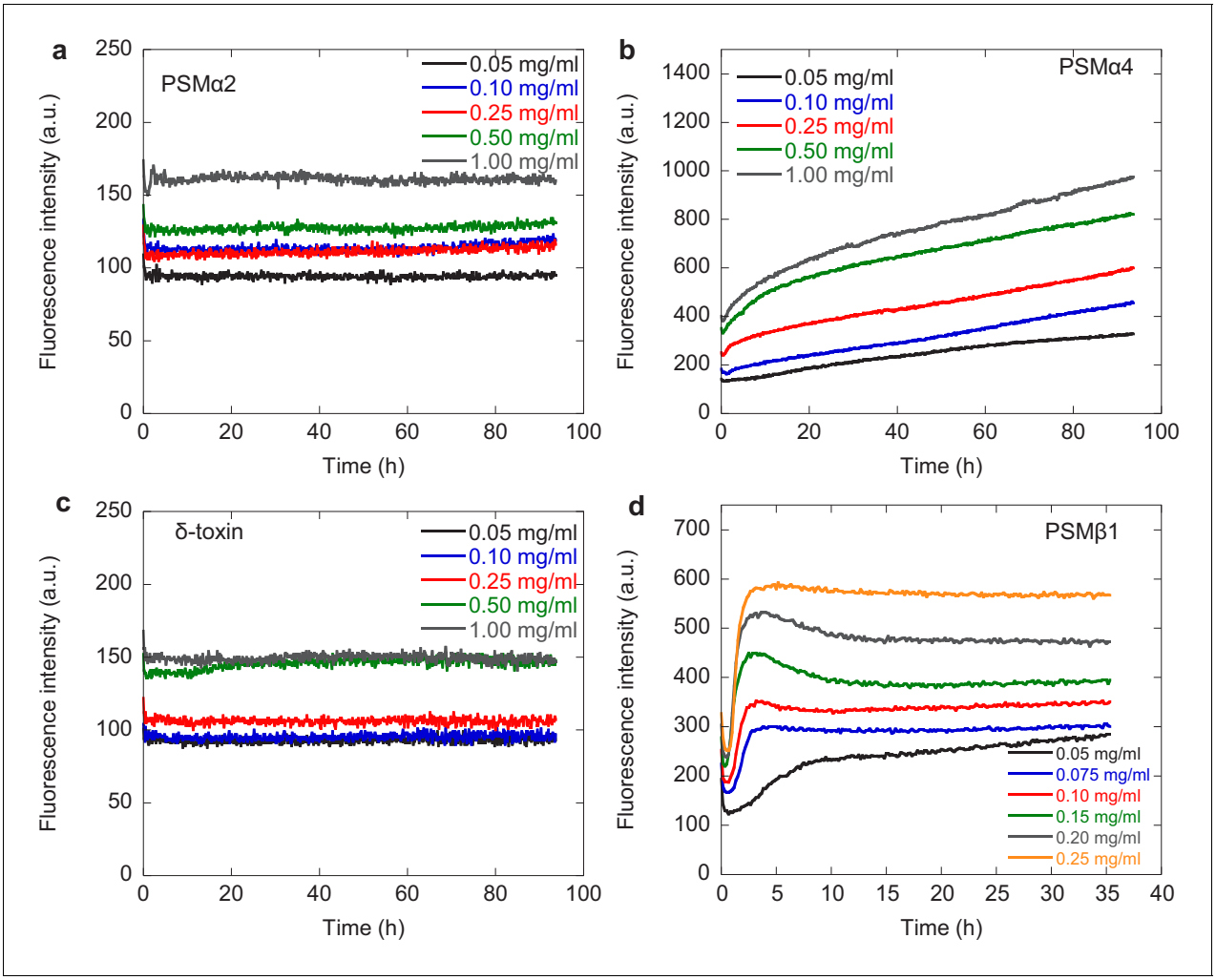

Figure 1—figure supplement 2. Kinetic data for phenol-soluble modulin (PSM)α2, PSMα4, δ-toxin, and PSMβ1. Experimental kinetic data for the aggregation of the PSMs peptides under quiescent conditions. Aggregation of PSM peptides (**a**) PSMα2, (**b**) PSMα4, (**c**) δ-toxin, and (**d**) PSMβ1 from monomeric samples (0.05–0.25 mg/mL) is measured by ThT fluorescence at 37°C every 10 min. Three repeats were carried out at each condition. At higher concentrations of PSMβ1 the lag-time becomes independent of the monomer concentration indicating some sort of saturation effect.

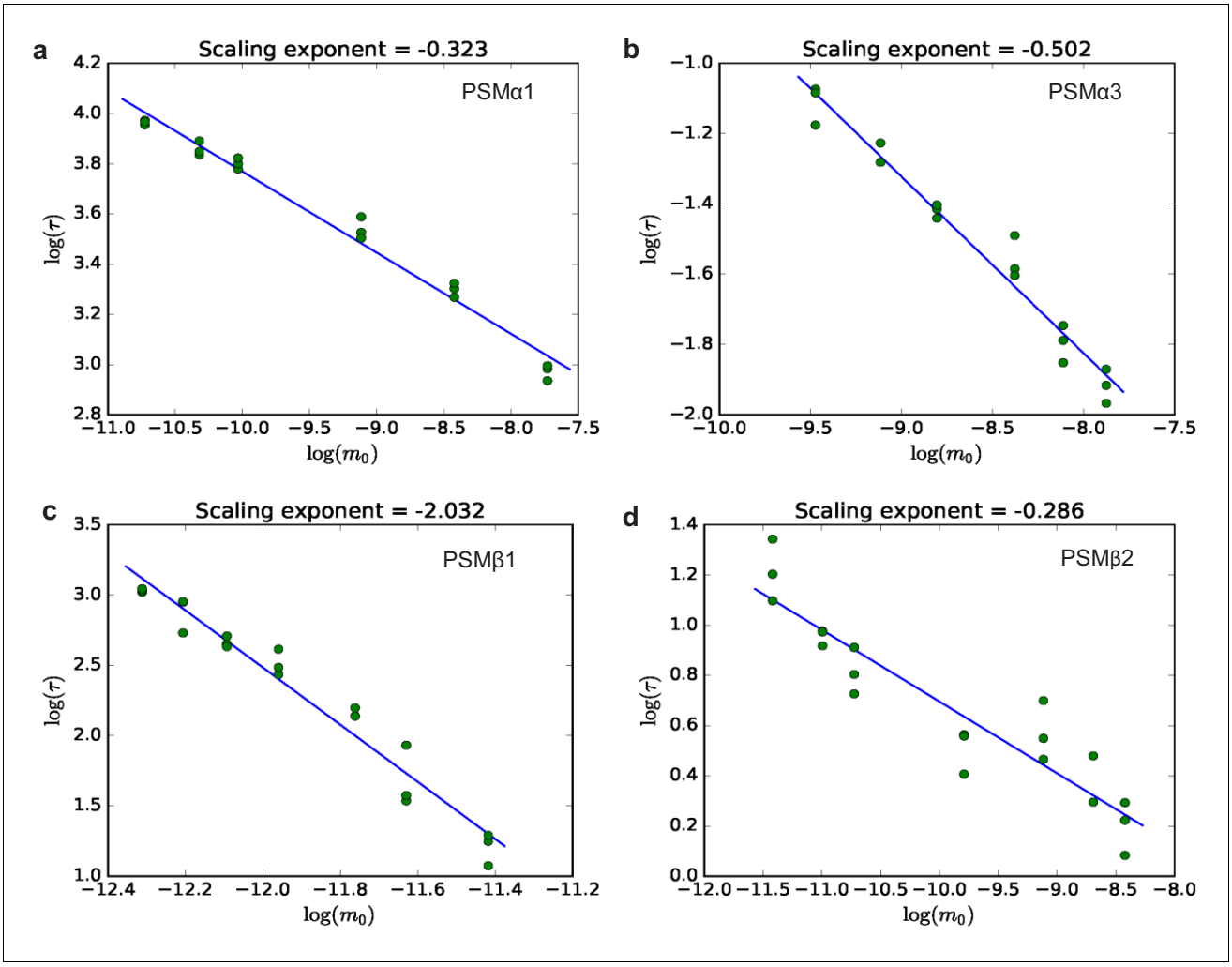

Figure 1—figure supplement 3. Half-time plots for phenol-soluble modulin (PSM)α1, PSMα3, PSMβ1, and PSMβ2. The half times of fibril formation as a function of initial monomer concentration on double logarithmic axes. The slope of the fitted line gives the scaling exponent (γ), obtained from three repeats of the aggregation experiments for each peptide. (**a**) PSMα1, (**b**) PSMα3, (**c**) PSMβ1, and (**d**) PSMβ2. The straight line in all four plots indicates that the dominant mechanism of fibril multiplication is the same for all monomer concentrations for the individual peptides studied here.

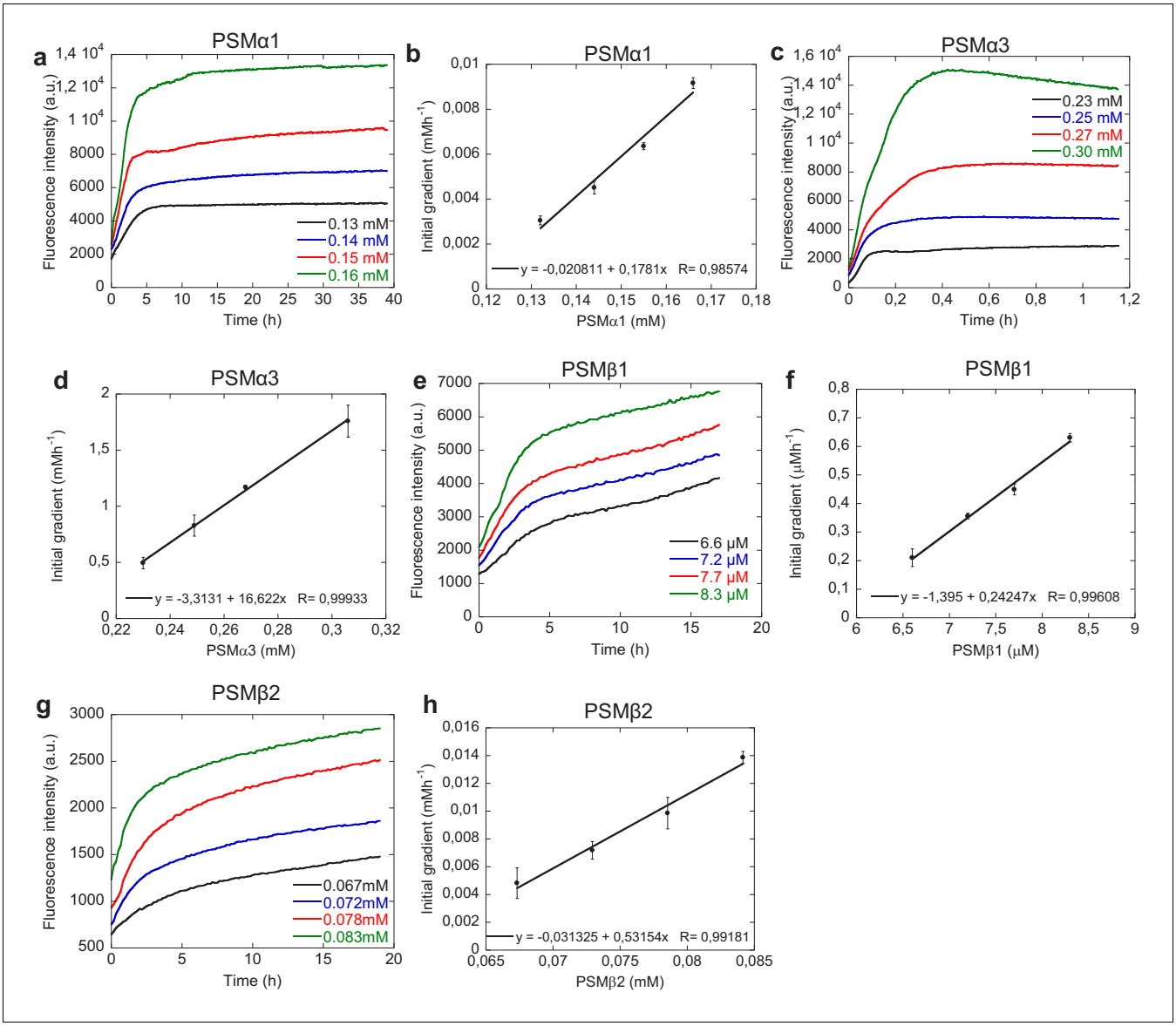

Figure 1—figure supplement 4. Seeding with high amounts of seeds. Seeding of phenol-soluble modulin (PSM) peptides with 20–50% preformed fibrils seeds (in monomeric equivalents) at different monomeric concentration. (**a**) Changes in ThT fluorescence when monomeric PSMα1 at fixed concentration (0.25 mg/mL) was incubated in the presence of high concentrations of preformed fibrils from the PSMα1 under quiescent conditions at 37˚C. (**b**) Initial gradient of the ThT fluorescence curves of PSMα1 used to estimate the elongation rates. The initial gradient (first 120 min) is plotted against the free monomer concentration. A straight line was fitted to these points, with the slope proportional to the number of seed fibrils and the elongation rate constant. (**c**) Changes in ThT fluorescence when monomeric PSMα3 at fixed concentration (0.5 mg/mL) was incubated in the presence of high concentrations of preformed fibrils from the PSMα3 under quiescent conditions at 37˚C. (**d**) Initial gradient of the ThT fluorescence curves of PSMα3 used to estimate the elongation rates. The initial gradient (first 2 min) is plotted against the free monomer concentration. A straight line was fitted to these points, with the slope proportional to the number of seed fibrils and the elongation rate constant. (**e**) Changes in ThT fluorescence when monomeric PSMβ1 at fixed concentration (0.025 mg/mL) was incubated in the presence of high concentrations of preformed fibrils from the PSMβ1 under quiescent conditions at 37˚C. (**f**) Initial gradient of the ThT fluorescence curves of PSMβ1 used to estimate the elongation rates. The initial gradient (first 120 min) is plotted against the free monomer concentration. A straight line was fitted to these points, with the slope proportional to the number of seed fibrils and the elongation rate constant. (**g**) Changes in ThT fluorescence when monomeric PSMβ2 at fixed concentration (0.25 mg/mL) was incubated in the presence of high concentrations of preformed fibrils and the PSMβ2 under quiescent conditions at 37˚C. (**h**) Initial gradient of the ThT fluorescence curves of PSMβ2 used to estimate the elongation rates. The initial gradient (first 120 min) is plotted against the free monomer concentration. A straight line was fitted to these points, with the slope proportional to the number of seed fibrils and the elongation rate constant.

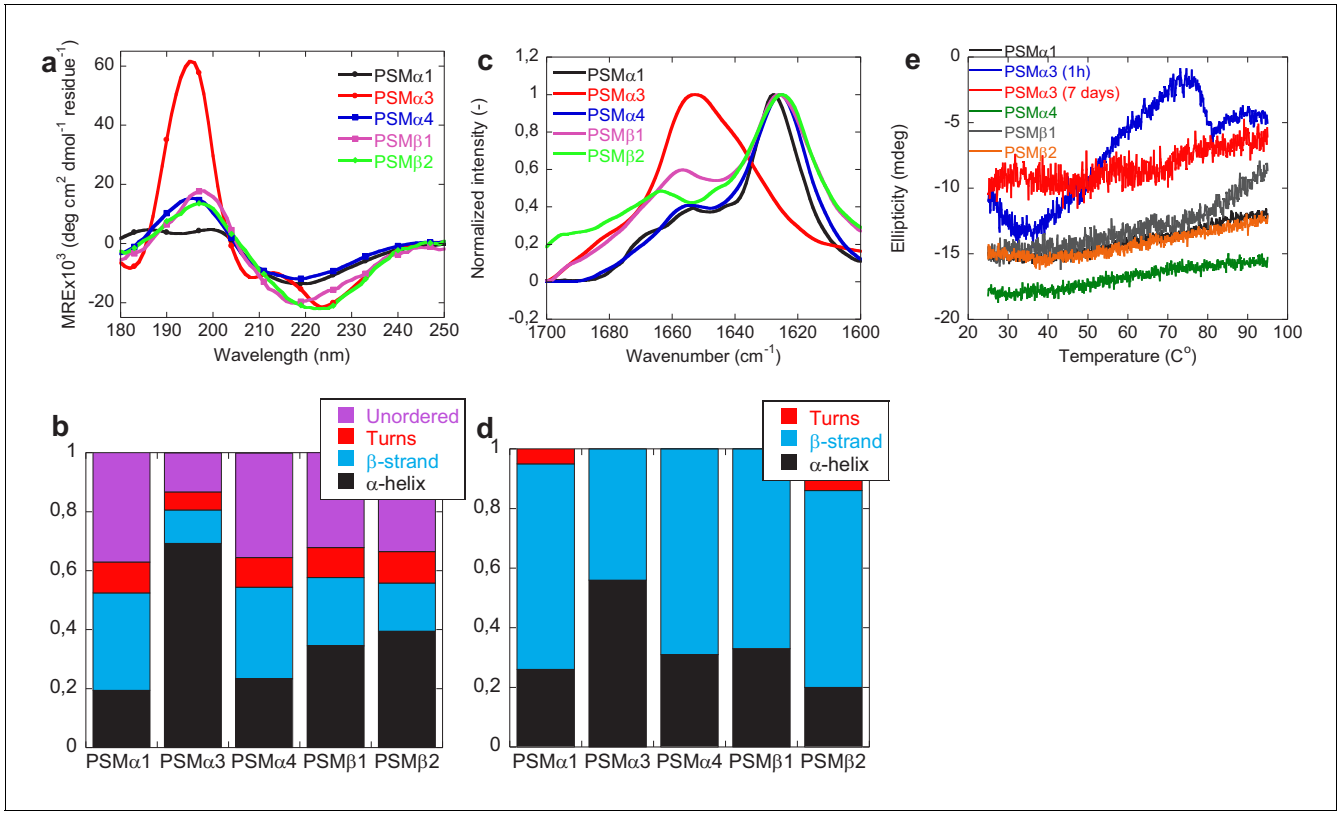

Figure 2. Structural comparison of fibrils formed by different phenol-soluble modulins (PSMs) variants. (**a**) Synchrotron radiation (SR) far UV-CD spectra of PSMα1, PSMα3, PSMα4, PSMβ1, and PSMβ2 fibrils recorded after 7 days of incubated samples except for PSMα3 which is recorded after 1 hr of incubated samples. (**b**) Deconvolution of the SRCD spectra of fibrils of PSM variants into the individual structural components. (**c**) Fourier transform infrared (FTIR) spectroscopy of the amide I' region (1600–1700 cm^{-1}) of fibrils of PSMs variants. PSMα1, PSMα4, PSMβ1, and PSMβ2 show a peak at 1625 cm^{-1} corresponding to rigid amyloid fibrils. In contrast, PSMα3 shows a peak at and 1654 cm^{-1}indicating α-helical structure in the fibrils. (**d**) Deconvolution of the FTIR spectra of fibrils of the PSM variants into the individual structural components. (**e**) CD (Jasco) thermal scans from 20°C to 95°C of PSMα1, PSMα3 (1 hr), PSMα3 (7 days), PSMα4, PSMβ1, and PSMβ2 fibrils.

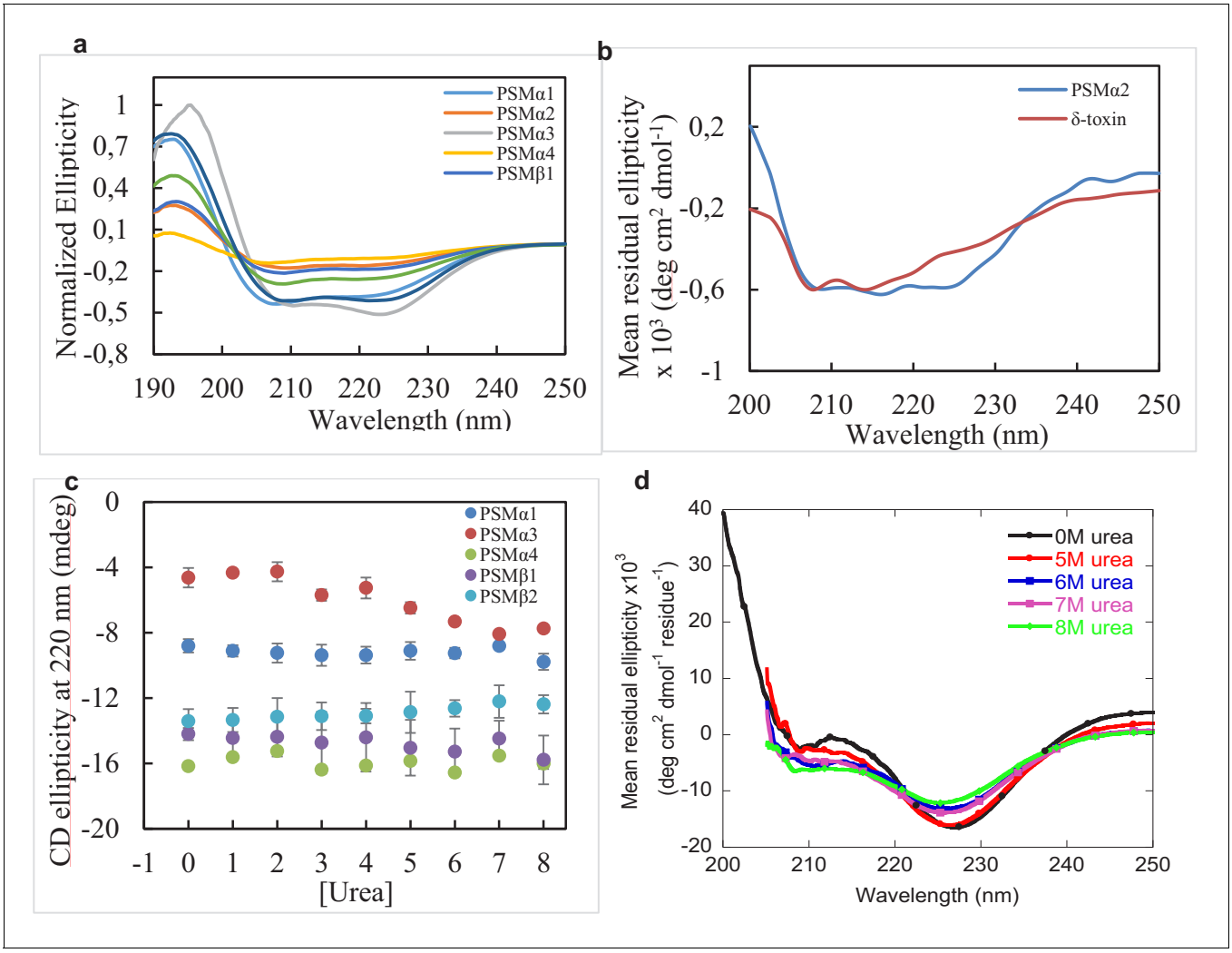

Figure 2—figure supplement 1. CD spectra of monomeric phenol-soluble modulin (PSM) peptides and urea denaturation of PSM fibrils. CD spectra (Jasco) of monomeric PSM peptides and of PSM peptides that do not aggregate. (**a**) CD spectra of monomeric PSMs peptides (0.25 mg/mL) measured at 25˚C followed by 0 hr of incubation period. (**b**) Far UV-CD spectra of PSMα2 and δ-toxin after 7 days of incubation at 37˚C display α-helical character consistent with the lack of aggregation. (**c**) Analysis of the dissociation of PSMs fibrils collected from plate reader experiments after incubation in the presence of various concentrations of urea (0–8M). (**d**) Far UV-CD (Jasco) spectra of PSMα3 fibrils (1 hr) after incubation in the absence and presence of high concentrations of urea (0 and 5–8 M urea).

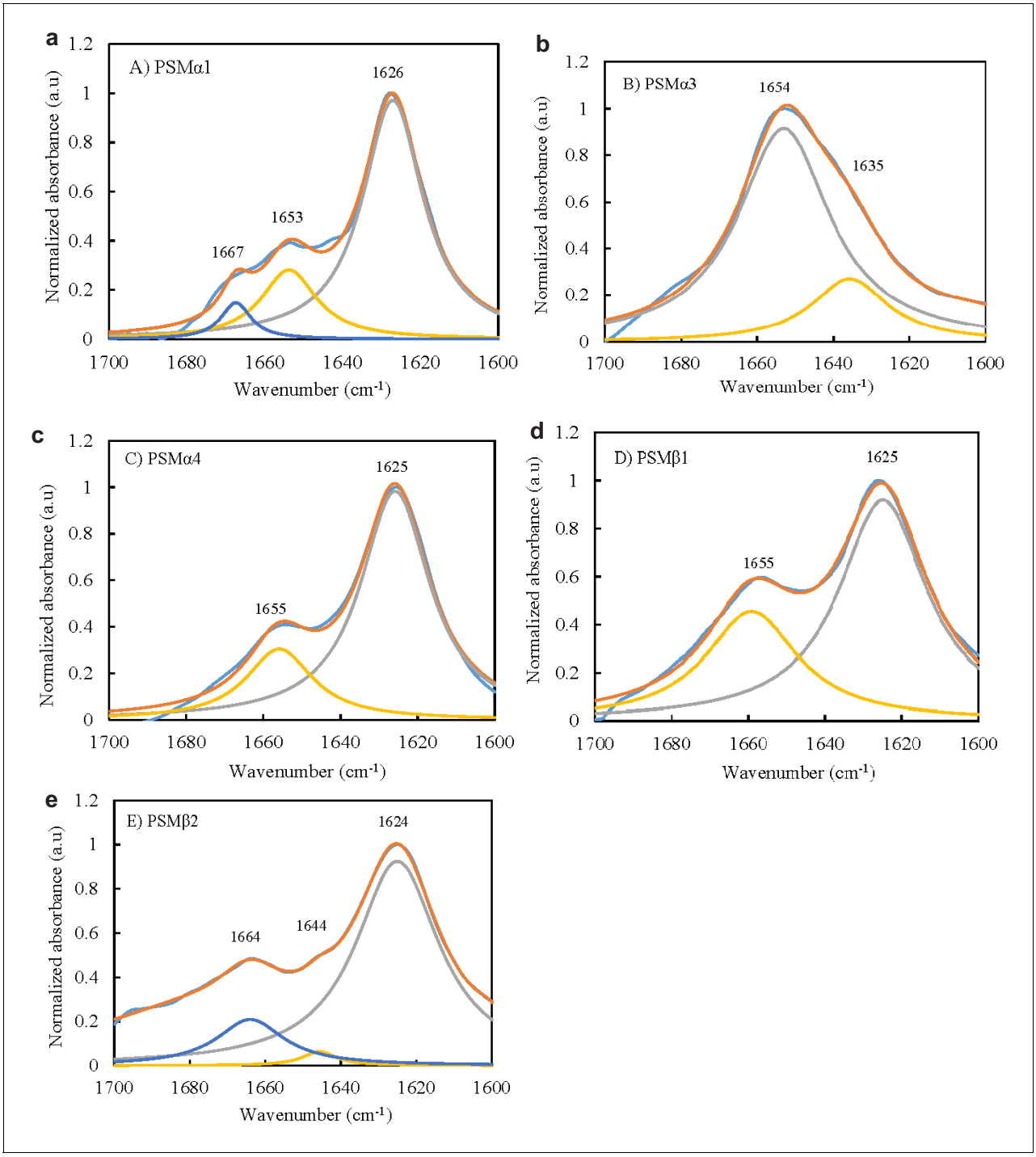

Figure 2—figure supplement 2. Deconvolution of Fourier transform infrared (FTIR) spectra. FTIR analysis of the secondary structure of phenol-soluble modulin (PSM) peptides. The data were processed by baseline correction and interfering signals from H_2O and CO_2 were removed using the atmospheric compensation filter. Further, peak positions were assigned where the second order derivative had local minima and the intensity was modeled by Gaussian curve fitting using the OPUS 5.5 software. (**a**) FTIR spectra and second order derivative of the spectra of PSMα1 at 0.5 mg/mL. (**b**) FTIR spectra and second order derivative of the spectra of PSMα3 at 0.5 mg/mL. (**c**) FTIR spectra and second order derivative of the spectra of PSMα4 at 0.5 mg/mL. (**d**) FTIR spectra and second order derivative of the spectra of PSMβ1 at 0.025 mg/mL. (**e**) FTIR spectra and second order derivative of the spectra of PSMβ2 at 0.25 mg/mL.

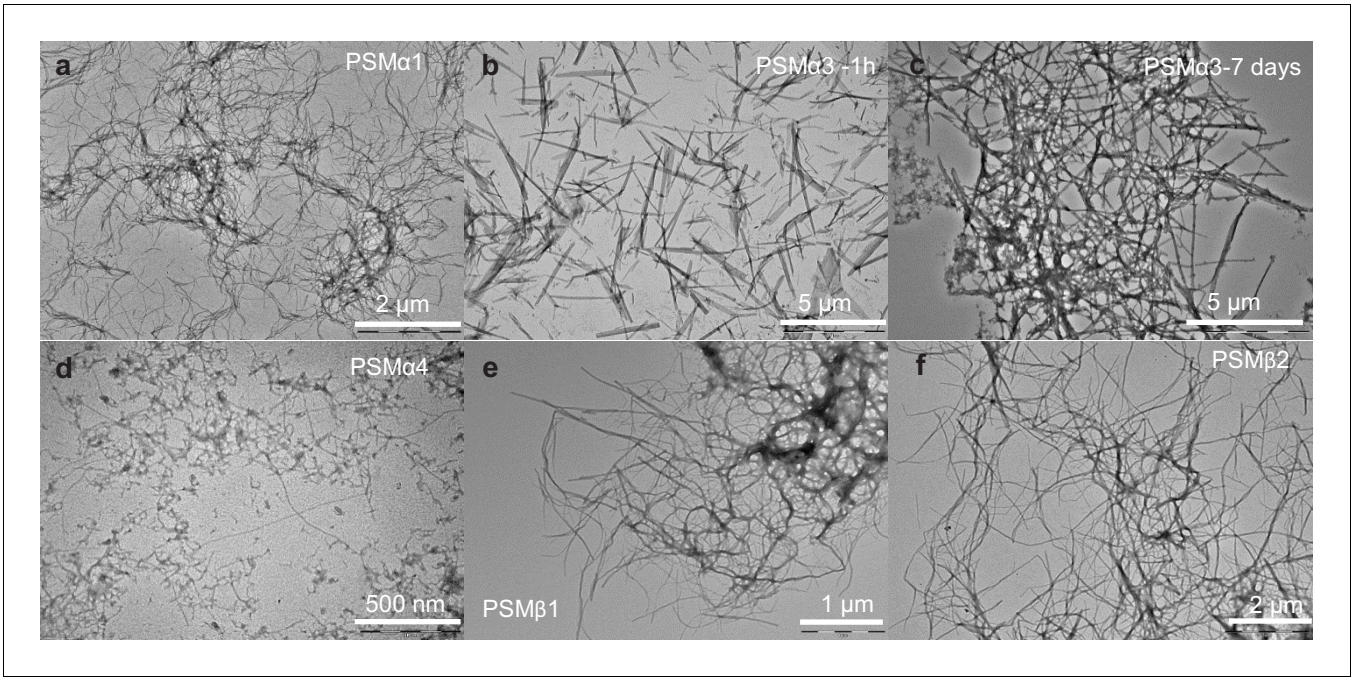

Figure 3. Morphology of aggregates of phenol-soluble modulin (PSMs) peptides. Transmission electron microscopic image of the end state of reaction for samples initially composed of (**a**) PSMα1 fibrils, (**b**) PSMα3 fibrils after 1 hr of incubation, (**c**) PSMα3 fibrils after 7 days of incubation, (**d**) PSMα4 fibrils, (**e**) PSMβ1 fibrils, and (**f**) PSMβ2 fibrils. Please note that scale bar changes.

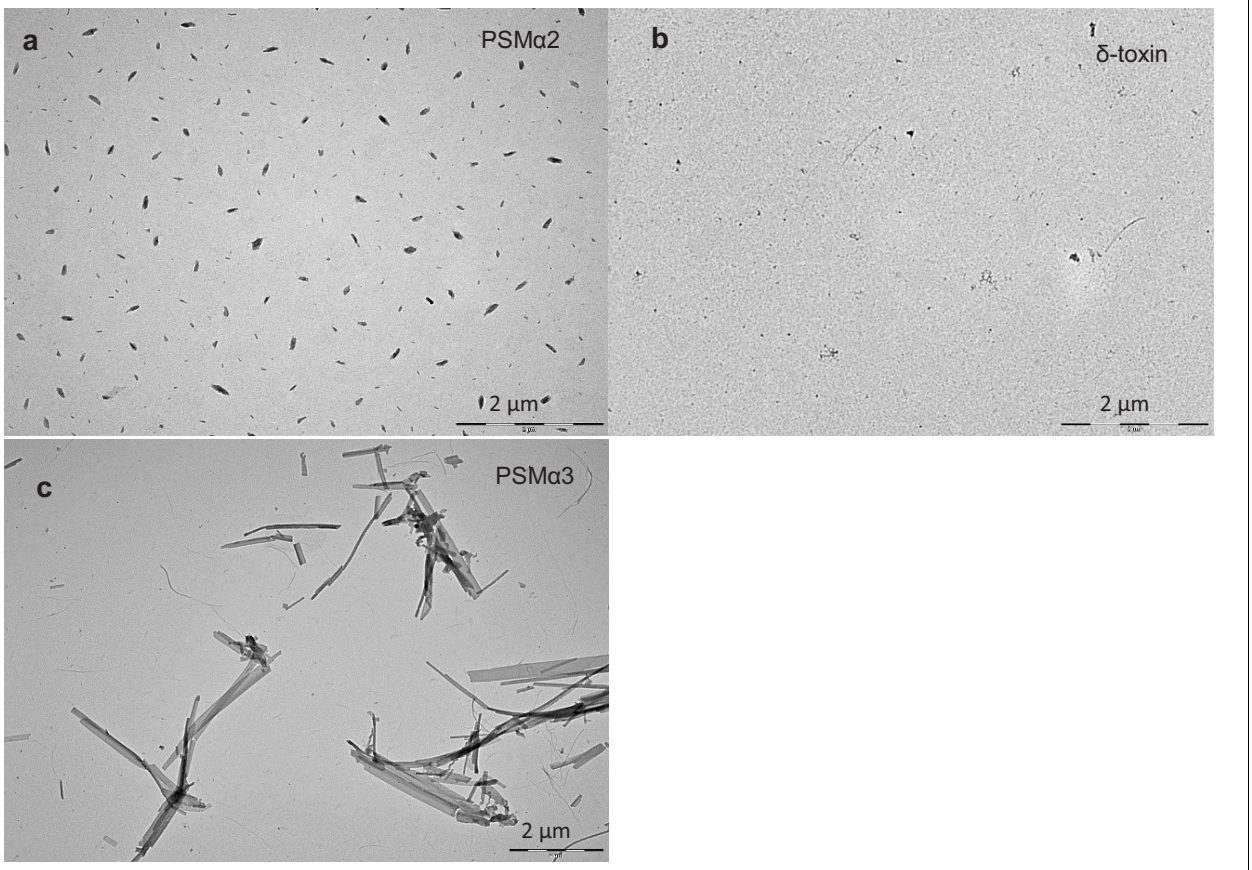

Figure 3—figure supplement 1. Morphology of phenol-soluble modulins (PSMs) peptides. Transmission electron microscopic image of the end state of reaction for samples initially composed of (**a**) PSMα2 monomers, (**b**) δ-toxin monomers, and (**c**) PSMα3 after 2 days of incubation.

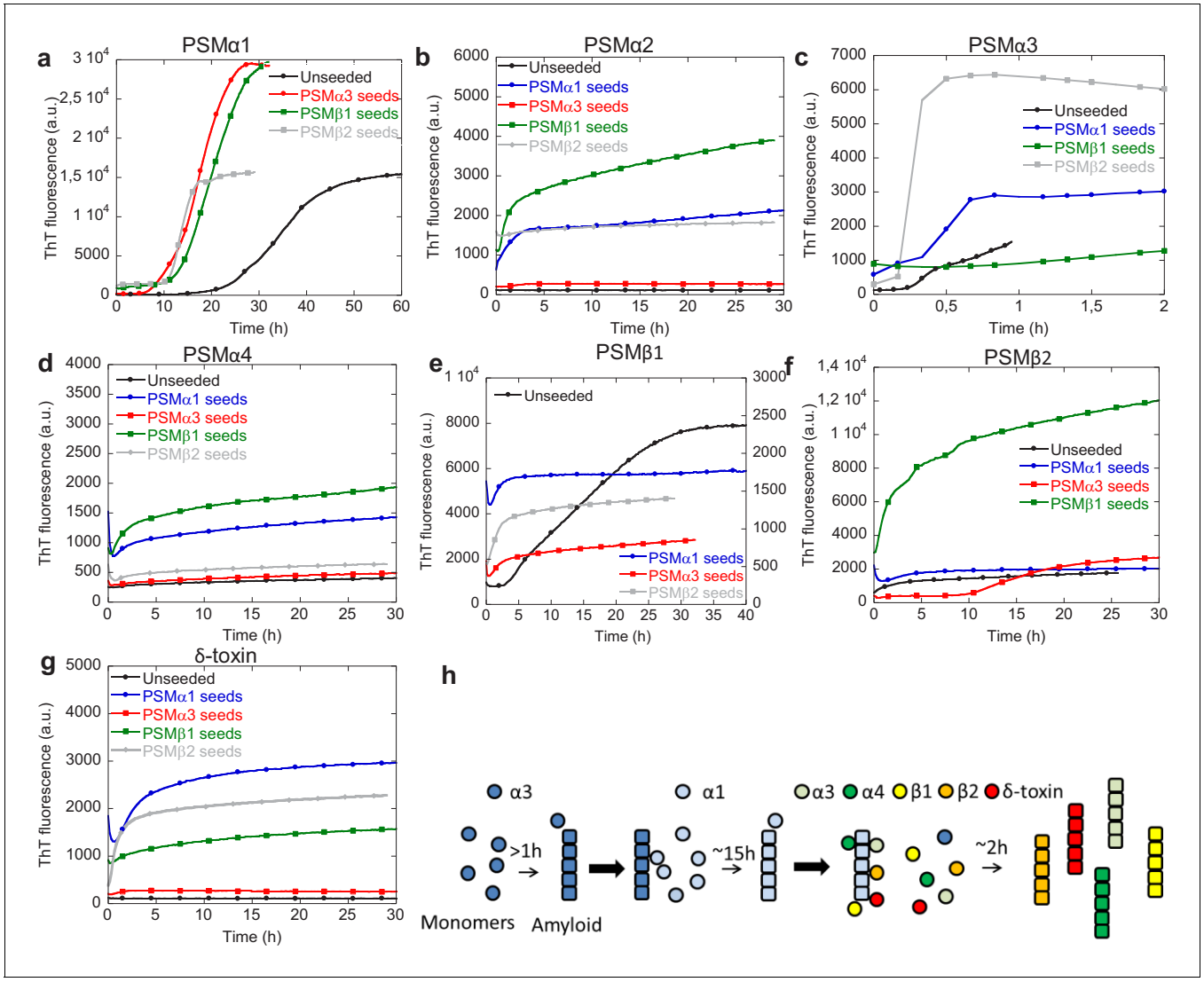

Figure 4. Cross-seeding phenol-soluble modulins (PSMs) variant. (**a**) Aggregation of PSMα1 (0.25 mg/mL) in the absence of seeds and in the presence of 20% (20 μM) preformed PSMα3 seeds, PSMβ1 seeds, and PSMβ2 seeds. (**b**) Aggregation of PSMα2 (0.25 mg/mL) in the absence of seeds and in the presence of 20% (20 μM) preformed PSMα1 seeds, PSMα3 seeds, PSMβ1 seeds, and PSMβ2 seeds. (**c**) Aggregation of PSMα3 (0.25 mg/mL) in the absence of seeds and in the presence of 20% (20 μM) preformed PSMα1 seeds, PSMβ1 seeds, and PSMβ2 seeds. (**d**) Aggregation of PSMα4 (0.25 mg/mL) in the absence of seeds and in the presence of 20% (20 μM) preformed PSMα1 seeds, PSMα3 seeds, PSMβ1 seeds, and PSMβ2 seeds. (**e**) Aggregation of PSMβ1 (0.025 mg/mL) in the absence of seeds and in the presence of 20% (1 μM) preformed PSMα1 seeds, PSMα3 seeds, and PSMβ2 seeds. (**f**) Aggregation of PSMβ2 (0.25 mg/mL) in the absence of seeds and in the presence of 20% (10 μM) preformed PSMα1 seeds, PSMα3 seeds, and PSMβ1 seeds. (**g**) Aggregation of δ-toxin (0.25 mg/mL) in the absence of seeds and in the presence of 20% (20 μM) preformed PSMα1 seeds, PSMα3 seeds, PSMβ1 seeds, and PSMβ2 seeds. (**h**) Schematic representation of the cross-seeding interactions between the PSM variants during biofilm formation.

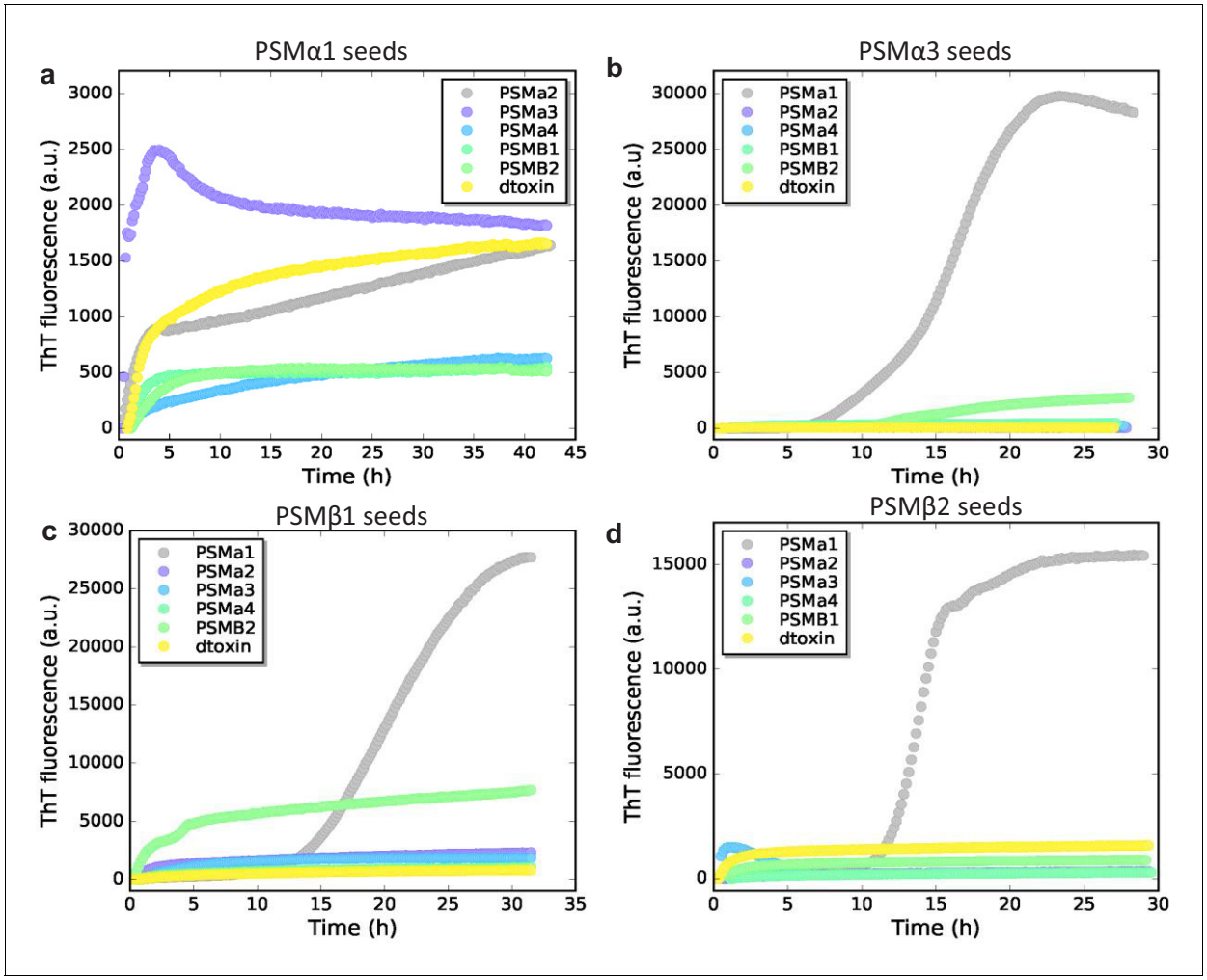

Figure 4—figure supplement 1. Cross-seeding of phenol-soluble modulin (PSM) peptides based on seed type. (**a**) Aggregation of PSMα2, PSMα3, PSMα4, PSMβ1, PSMβ2, and δ-toxin (0.25 mg/mL) in the presence of 20% preformed PSMα1 seeds. (**b**) Aggregation of PSMα1, PSMα2, PSMα4, PSMβ1, PSMβ2, and δ-toxin (0.25 mg/mL) in the presence of 20% preformed PSMα3 seeds. (**c**) Aggregation of PSMα1, PSMα2, PSMα3, PSMα4, PSMβ2, and δ-toxin (0.25 mg/mL) in the presence of 20% preformed PSMβ1 seeds. (**d**) Aggregation of PSMα1, PSMα2, PSMα3, PSMα4, PSMβ1, and δ-toxin (0.25 mg/mL) in the presence of 20% preformed PSMβ2 seeds.

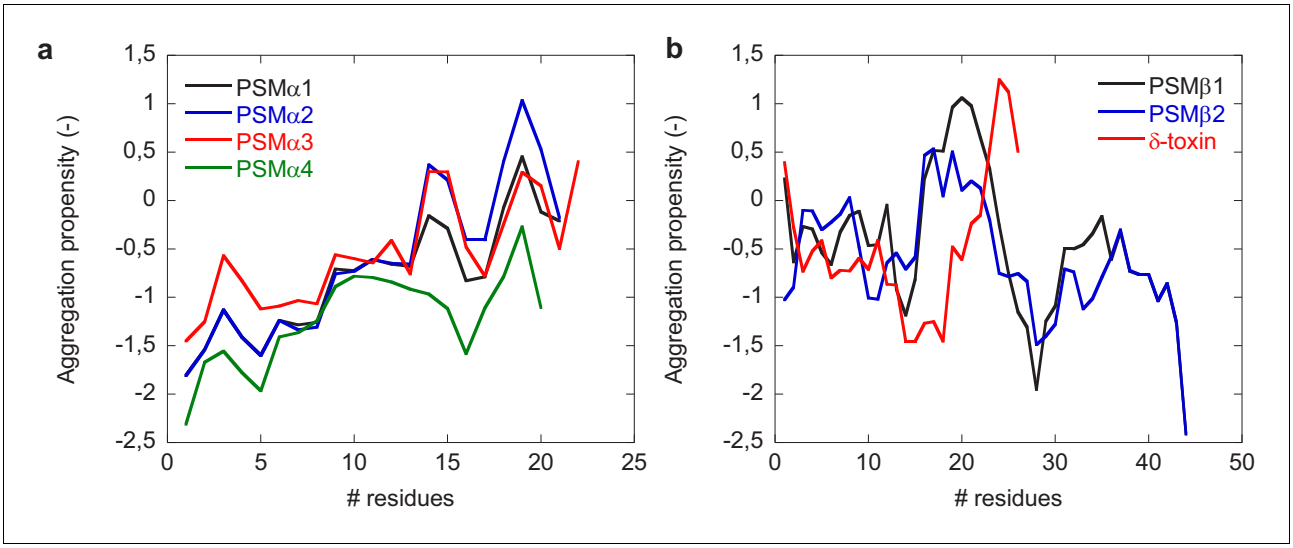

Figure 4—figure supplement 2. Aggregation propensity profiles of phenol-soluble modulin (PSM) peptides using CamSol. (**a**) Aggregation propensities of PSMα group of peptides (PSMα1, PSMα2, PSMα3, and PSMα4). (**b**) Aggregation propensity of PSMβ group of peptides (PSMβ1 and PSMβ2) along with δ-toxin.